Pulmonary adenofibroma with central liquefaction necrosis: A case report

RUXIN SHEN[1], LILI SHE[2] and ZHAOSHUI LI[3]

Departments of [1]Thoracic Surgery and [2]Pathology, The Sixth People's Hospital of Nantong, Nantong,
Jiangsu 226000; [3]Qingdao Medical College, Qingdao University, Qingdao, Shandong 266000, P.R. China

Abstract. Pulmonary adenofibroma (PAF) is a rare benign tumor. Computed tomography (CT) imaging of PAF show well-defined, homogeneous and solitary nodules. To the best of our knowledge, there is no report of PAF presenting with central liquefaction necrosis on CT images. The present study reports the case of a 70-year-old man who was hospitalized due to an inguinal hernia without respiratory symptoms. Chest CT scan revealed a tumor (~6.5x5.5x4.4 cm) in the lower lobe of the left lung, characterized by uneven density and unclear boundary with the pleura. Contrast-enhanced scan revealed that the lesion was slightly enhanced and liquefaction necrosis appeared in its center. Wedge resection was performed using video-assisted thoracic surgery. Histopathological and immunohistochemical examination confirmed the diagnosis of PAF.

Introduction

Pulmonary adenofibroma (PAF) is a rare benign tumor, with ~40 cases reported worldwide since 1944 (1). It is not listed in the 5th edition of the World Health Organization (WHO) classification of thoracic tumors (2). Although there is no unified consensus, it is considered that PAF is a benign tumor (3). Whether PAF and pulmonary solitary fibrous tumor (PSFT) are homologous remains controversial, but differential diagnosis is necessary (4). In most cases, computed tomography (CT) imaging of PAF shows well-defined, homogeneous and solitary nodules which cannot be easily differentiated from PSFT. To the best of our knowledge, the present study is the first report of a patient with PAF with liquefaction necrosis in the center of the tumor on CT.

Correspondence to: Dr Ruxin Shen, Department of Thoracic Surgery, The Sixth People's Hospital of Nantong, 881 Yonghe Road, Nantong, Jiangsu 226000, P.R. China
E-mail: drshenruxin@yeah.net

Case report

A 70-year-old man was hospitalized with an inguinal hernia at The Sixth People's Hospital of Nantong (Nantong, China) on July 5, 2021. The patient did not have any respiratory symptoms or discomfort. Chest CT scan revealed a tumor (~6.5x5.5x4.4 cm) in the lower lobe of the left lung, characterized by uneven density and unclear boundary with the pleura and diaphragm. A contrast-enhanced scan demonstrated a slightly enhanced lesion with liquefaction necrosis in the center (Fig. 1). The results of tumor markers, including α fetoprotein, carcinoembryonic antigen, carbohydrate antigen 125, carbohydrate antigen 19-9, carbohydrate antigen 72-4, carbohydrate antigen 50, neuron specific enolase, cytokeratin 19 fragment, pro-gastrin-releasing peptide and serum ferritin, were within the normal range. Initially, a benign lung tumor was suspected although malignant tumor could not be ruled out. The patient and his family refused needle biopsy and preferred surgical resection of the tumor. Therefore, the patient underwent video-assisted thoracic surgery (VATS). An intraoperative assessment revealed that the tumor was localized at the bottom of the left lower lobe, with an intact capsule and smooth surface. The tumor partly invaded the lung tissue and partly adhered to the diaphragm (Fig. 2). Thus, wedge resection of the left lung lower lobe was performed to ensure complete tumor removal via VATS. The result of intraoperative frozen section showed a benign tumor. Postoperative pathology revealed that the tumor comprised epithelial and stromal spindle cells. The cubic epithelial cells covered the tumor, forming gland-like fissures. The central tissue of the tumor was decomposed and liquefied, normal cell structure disappeared and a large number of foam cells were seen. The epithelial cells only covered the tumor surface and adenoid fissures. Foam cells were only visible in part of the central liquefied necrotic area. The majority of the tumor was composed of stromal cells. Due to the large size of the tumor, some low-quality sections were generated during the processing of specimen fixation, pathological sampling and paraffin embedment. Therefore the analysis of the percentage of epithelial, stromal and foam cells was affected by large errors. Immunohistochemistry demonstrated that the epithelial component stained positive for pan-cytokeratin and epithelial membrane antigen and the stromal component stained positive for Bcl-2, CD34, STAT6 and vimentin. The tumor showed negative staining for CD99, estrogen and progesterone receptor, desmin, S100, smooth muscle actin and thyroid

transcription factor 1 markers (Fig. 3). Tumor tissues were fixed in 10% neutral buffered formalin at 4˚C for 24 h. Sections were cut from paraffin-embedded blocks at a thickness of 3 μm. At room temperature, sections were stained with hematoxylin and eosin for 6 min for histopathological analysis. A Leica Bond MAX automated immunostainer (Leica Biosystems) was used for immunostaining. Paraffin-embedded sections were placed in xylene I and xylene II, respectively, for 10 min. After removing excess fluid, sections were placed in absolute ethanol I and absolute ethanol II, respectively, for 2 min, 95% ethanol for 2 min, 75% ethanol for 2 min, distilled water for 2 min and phosphate buffered solution (PH 7.3). Slides were heated in elhylene diamine tetraacetic acid antigen repair buffer (pH 8.0) for 20 min at 95˚C to retrieve the antigens. Sections were rinsed with phosphate buffered solution (PH 7.3) three times after natural cooling (2 min per rinse). The endogenous peroxidase was blocked with 3% hydrogen peroxide for 10 min at room temperature. Sections were incubated with primary antibodies (ready-to-use) overnight at 4˚C. The endogenous peroxidase was blocked with 3% hydrogen peroxide for 8 min at room temperature. Subsequently, sections were incubated with the secondary antibody (ready-to-use) for 8 min at room temperature. Chromogen detection was performed using a DAB detection kit (polymer) (ready-to-use; including endogenous peroxidase, horseradish peroxidase-conjugated sheep anti-mouse or anti-rabbit IgG, DAB substrate buffer and DAB chromogen). The primary antibodies used were as follows: Monoclonal mouse anti-human pan-cytokeratin (ready-to-use; cat. no. ZM-0069), monoclonal mouse anti-human epithelial membrane antigen (ready-to-use; cat. no. ZM-0095), monoclonal mouse anti-human Bcl-2 (ready-to-use; cat. no. ZM-0536), monoclonal mouse anti-human CD34 (ready-to-use; cat. no. ZM-0046), polyclonal rabbit anti-human STAT6 (ready-to-use; cat. no. ZA-0647), monoclonal mouse anti-human vimentin (ready-to-use; cat. no. ZM-0260), monoclonal mouse anti-human CD99 (ready-to-use; cat. no. ZA-0577), monoclonal mouse anti-human estrogen receptor (ready-to-use; cat. no. ZA-0102), monoclonal mouse anti-human progesterone receptor (ready-to-use; cat. no. ZA-0255), monoclonal mouse anti-human desmin (ready-to-use; cat. no. ZA-0610), monoclonal mouse anti-human S100 (ready-to-use; cat. no. ZM-0224), monoclonal mouse anti-human smooth muscle actin (ready-to-use; cat. no. ZM-0003) and monoclonal mouse anti-human thyroid transcription factor 1 markers (ready-to-use; cat. no. ZM-0270) (all purchased from OriGene Technologies, Inc.). The secondary antibody Bond Polymer Refine Detection (ready-to-use; cat. no. DS9800-CN) (Leica Biosystems) was labeled with compact polymer. The sections were observed using an Olympus BX53 light microscope (Olympus Corporation; magnification, x40 or x200). The diagnosis of PAF was based on the epithelial and stromal cells and adenoid structures. Nine months after the operation, the patient was in good health, with no recurrence or metastasis.

Discussion

Currently, the pathogenesis of PAF is unclear (5). Clinical data has shown that most patients with PAF are middle-aged (1). Because of the slow progression of PAF, most patients do not show symptoms in the early stages. Suster and Moran (3)

demonstrated that PAF is a type of immature hamartoma based on its inability to differentiate into more specialized mature components, such as fat, smooth muscle or cartilage. Fusco *et al* (6) proposed that PAF is not only a benign tumor but a certain type of solitary fibrous tumor (SFT). By contrast, Lindholm *et al* (7) suggested that PAF should be not included in the SFT spectrum due to potential recurrence and metastasis of SFT. However, careful analysis should be conducted to distinguish PAF from PSFT because they exhibit a degree of homology.

PAF comprises stromal and epithelial components and is characterized by a biphasic growth pattern due to the growth of these two components (8). Histopathologically, PAF is characterized by the presence of stromal cells and gland-like fissures covered with epithelial cells. PSFT is an intermediate tumor and is listed as a tumor of fibroblastic/myofibroblastic differentiation in the 5th edition of WHO classification of thoracic tumors (2). PSFT has a similar stromal composition to PAF. PSFT consists of dense and sparse areas of cells with collagen fibers between the two areas (8). Based on these typical features, PAF was diagnosed in the present case. Atypical histopathological findings make it difficult to perform a differential diagnosis for PAF and PSFT. Therefore, immunohistochemistry should be performed.

In most cases, PAF manifests as well-circumscribed isolated nodules in the peripheral lung (1). However, fat, cartilage or calcification do not appear in the lesions (9). In the present case, the enhanced CT scan showed mild or moderate enhancement because PAF primarily comprises stromal and epithelial cells with limited blood supply. In contrast-enhanced CT scan of PSFT, the cell-dense and vascular-rich areas are significantly enhanced, while the cell-sparse and low-vascular areas are not significantly enhanced (10). Based on the aforementioned facts, we hypothesized that PAF and PSFT present as liquefaction necrosis of certain tumors due to large tumor size and poor blood supply. There is evidence of cavitation in PAF in the center of the tumor (8). These characteristics make difficult to reach a conclusive diagnosis. Additionally, there is a need to differentiate PAF from other malignant tumors such as carcinosarcoma and pleuropulmonary blastoma on CT images (11). Due to non-specific imaging findings of PAF, the diagnosis and differentiation from other tumors, especially PSFT, is based on histopathology and immunohistochemistry (12).

In addition, both PAFs and PSFTs contain stromal elements, hence both may test positive for CD34, CD31, Bcl-2, CD99 and vimentin (6). PSFT is mainly positive for STAT-6, CD34 and BCL-2 expression (13). On the other hand, PAF is typically negative for STAT6 expression, and only a proportion of patients show positivity for CD34 and Bcl-2. For example, Liang *et al* (1) reported patients who showed positive expression of CD34 (14/33) and Bcl-2 (11/26). In the study by Lindholm *et al* (7), 13 patients with PAF showed no expression of CD34 and BCL-2. Analysis of nuclear expression demonstrated that STAT6 is a highly sensitive and specific marker of PSFT (14). Nonetheless, Fusco *et al* (6) found that PAF is a tumor with the molecular signature of SFT by finding a fusion gene of NAB2 exon 4 and STAT6 exon 2 in the stromal cells of both tumors. This finding may explain the positive staining of STAT6 in 5 out of 7 patients in their study. Similar results were extremely rare in previous reports. Both the present case
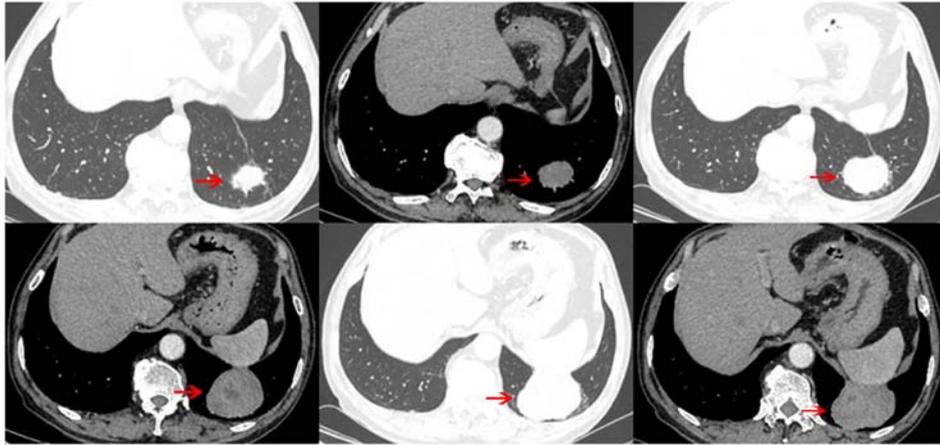
Figure 1. Slightly enhanced tumor, with liquefaction necrosis in the center (arrows indicate the tumor).
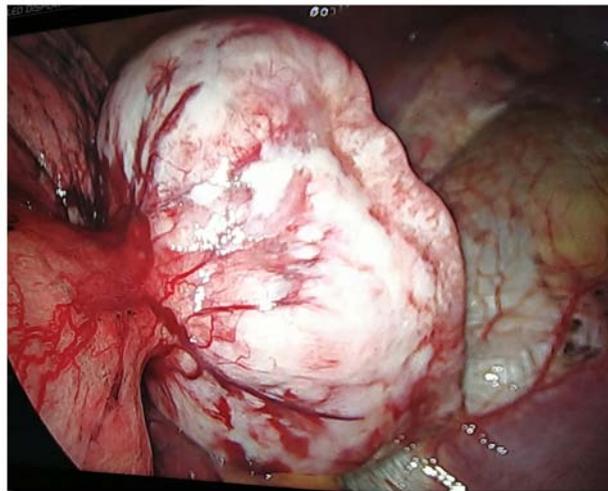
Figure 2. Tumor location during intraoperative examination. The tumor was localized at the bottom of the left lower lobe, with an intact capsule and smooth surface. The tumor partly invaded the lung tissue and partly adhered to the diaphragm.
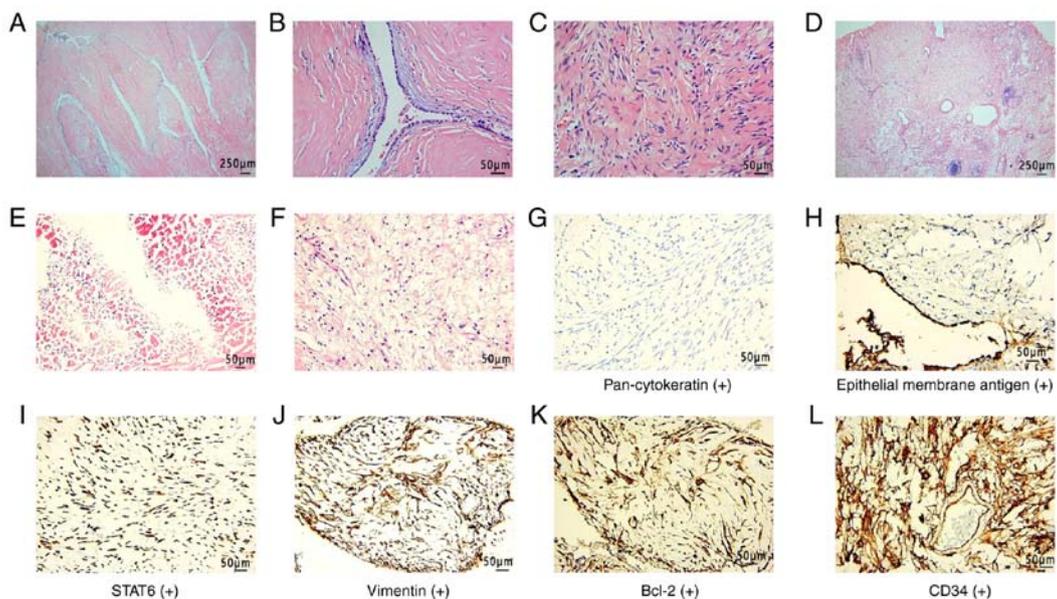
Figure 3. Histopathological and immunohistochemical results. (A and B) Mild cubic epithelial cells covered the tumor and formed gland-like fissures. (C) Stroma of the tumor comprising spindle cells. (D-F) Tissue decomposed and liquefied and cell structure disappeared. Numerous foam cells were seen. (G-L) Positive staining for pan-cytokeratin and epithelial membrane antigen, STAT6, vimentin, Bcl-2 and CD34, respectively

report and the case reported by Sonokawa *et al* (15) support the conclusion of Fusco *et al*.

Asymptomatic patients with small nodules do not require treatment but regular follow-up (9). For patients with symptoms, large tumors or difficult diagnosis lung biopsy can be performed according to the situation and clinical considerations. VATS is an appropriate approach for the diagnosis and treatment of PAF based on the present case.

Although biliary adenofibroma is associated with malignant transformation and lung metastasis (16), to the best of our knowledge there is no report of PAF metastasis or recurrence.

CT manifestations of PAF are not specific. Large PAF may present liquefaction necrosis due to poor central blood supply. This requires PAF to be distinguished from PSFT and malignant tumors on CT. Therefore, the final diagnosis is based on histopathology and immunohistochemistry.

Acknowledgements

Funding

Availability of data and materials

The datasets used and/or analyzed during the current study are available from the corresponding author on reasonable request.

Authors' contributions

RS drafted the manuscript. LS performed histopathological and immunohistochemical examination of the tumor. ZL collected patient data. RS, LS and ZL contributed to data analysis, drafting and revision of the manuscript. RS and LS confirm the authenticity of all the raw data. All authors have read and approved the final manuscript.

Ethics approval and consent to participate

This study was approved by the Ethics Committee of the Sixth People's Hospital of Nantong (approval No. 2022007).

Patient consent for publication

The patient provided oral informed consent for publication.

Competing interests

The authors declare that they have no competing interests.

References

1. Liang Z, Zhou P, Wang Y, Zhang Y, Li D, Su X, Fan Y, Tang Y, Jiang L and Wang W: Pulmonary adenofibroma: Clinicopathological and genetic analysis of 7 cases with literature review. Front Oncol 11: 667111, 2021.
2. WHO Classification of Tumours Editorial Board. WHO classification of tumours. Thoracic tumours. 5th edition. Vol. 5. Lyon: IARC Press, 2021.
3. Suster S and Moran CA: Pulmonary adenofibroma: Report of two cases of an unusual type of hamartomatous lesion of the lung. Histopathology 23: 547-551, 1993.
4. Erber R, Haller F, Hartmann A and Agaimy A: Prominent entrapment of respiratory epithelium in primary and metastatic intrapulmonary non-epithelial neoplasms: A frequent morphological pattern closely mimicking adenofibroma and other biphasic pulmonary lesions. Virchows Arch 477: 195-205, 2020.
5. Matsuda K, Nakajima W, Togashi T and Sano Y: Pulmonary adenofibroma in a sika deer. J Vet Med Sci 81: 486-490, 2019.
6. Fusco N, Guerini-Rocco E, Augello C, Terrasi A, Ercoli G, Fumagalli C, Vacirca D, Braidotti P, Parafioriti A and Jaconi M, *et al*: Recurrent NAB2-STAT6 gene fusions and oestrogen receptor-α expression in pulmonary adenofibromas. Histopathology 70: 906-917, 2017.
7. Lindholm KE, Sansano-Valero I, Rodriguez JL, Ramon Y and Moran CA: Pulmonary adenofibromas: A clinicopathologic correlation of 13 cases. Am J Surg Pathol 44: 917-921, 2020.
8. Hao J, Zhang C, Cao Q, Zou J and Wang C: Pulmonary adenofibroma: Report of a case with multiple masses. Ann Clin Lab Sci 46: 691-695, 2016.
9. Wang Y, Xiao HL, Jia Y, Chen JH, He Y, Tan QY and Zhang WG: Pulmonary adenofibroma in a middle-aged man: Report of a case. Surg Today 43: 690-693, 2013.
10. You X, Sun X, Yang C and Fang Y: CT diagnosis and differentiation of benign and malignant varieties of solitary fibrous tumor of the pleura. Medicine (Baltimore) 96: e9058, 2017.
11. Al-Amer M, Abdeen Y, Shaaban H and Alderink C: Solitary pulmonary adenofibroma in a middle-aged man with bladder cancer. Lung India 34: 570-572, 2017.
12. Rao N, Colby TV, Falconieri G, Cohen H, Moran CA and Suster S: Intrapulmonary solitary fibrous tumors: Clinicopathologic and immunohistochemical study of 24 cases. Am J Surg Pathol 37: 155-166, 2013.
13. Olson NJ, Czum JM, de Abreu FB, Linos K and Black CC: Synchronous pulmonary adenofibroma and solitary fibrous tumor: Case report and review of the literature. Int J Surg Pathol 27: 322-327, 2019.
14. Tan SY, Szymanski LJ, Galliani C, Parham D and Zambrano E: Solitary fibrous tumors in pediatric patients: A rare and potentially overdiagnosed neoplasm, confirmed by STAT6 immunohistochemistry. Pediatr Dev Pathol 21: 389-400, 2018.
15. Sonokawa T, Enomoto Y, Kunugi S, Terasaki Y and Usuda J: A case of pulmonary adenofibroma treated by thoracoscopic resection. J Nippon Med Sch 88: 564-568, 2021.
16. Akin O and Coskun M: Biliary adenofibroma with malignant transformation and pulmonary metastases: CT findings. AJR Am J Roentgenol 179: 280-281, 2002.